New Physics: Sae Mulli,
Vol. 69, No. 6, June 2019, pp. 649∼654
http://dx.doi.org/10.3938/NPSM.69.649

Critical Phenomena of the Generalized Epidemic Process

Meesoon Ha*
Department of Physics Education, Chosun University, Gwangju 61452, Korea

(Received 6 May 2019 : accepted 9 May 2019)

We investigate mixed-order critical phenomena of the generalized epidemic process (GEP) on random scale-free networks characterized by the power-law distribution $p_k \sim k^{-\alpha}$.The GEP is a minimal model of spreading behaviors. Near tricritical points (TCPs) derived by using the generating method, we numerically confirm the associated scaling exponents as functions of α. In particular, we propose an extended finite-size scaling theory of the GEP and crossover scaling behaviors, which are also confirmed by using extensive Monte Carlo simulations. Our results show that near TCPs, the GEP is governed by two distinct length scales, whose nontrivial dependence on α leads to rich transition behaviors.

PACS numbers: 02.50.-r, 05.70.Jk, 64.60.-i, 89.75.Hc
Keywords: GEP, Extended finite-size scaling, Mixed-order transitions, Tricriticality, Crossover scaling

I. introduction

Ranging from behavior adoption [1] to co-infection of multiple diseases [2], spreading phenomena are *complex contagions*, where multiple cooperating spreaders try to convert a common neighbor enhances or reduces the probability of success. These typically occur in systems with heterogeneous structure, *scale-free networks* characterizing by a power-law degree distribution with the probability that an arbitrary node is linked to k neighbors, $p_k \sim k^{-\alpha}$ [3]. Cooperative effects have been modeled in various ways. So far the bootstrap and k-core percolations [4,5] have received much attention as paradigmatic models describing the formation of a large-scale, highly-interconnected structure. The spreading dynamics has been more explicitly studied in terms of the Watts' threshold model [6], the generalized epidemic process (GEP) [7] and references therein, cooperative co-epidemics [8,9], two-step contagion model [10], and many others. All of these models show that, as contagion becomes more infectious, a singular transition occurs from a contagion-localized phase to an active phase where the contagion spreads to a finite fraction of the entire population. Moreover, as the strength of cooperation is increased, the type of the phase transition changes from continuous (the bond percolation) to discontinuous. The marginal case exhibits a continuous transition with two critical scaling fields. The GEP, similar to cooperative directed percolation [11, 12], illustrates nonequilibrium analogs of equilibrium tricritical points (TCPs) [13,14].

In this paper, we revisit mixed-order transitions of the GEP to discuss its phase diagrams with crossover scaling and the competition of relevant length scales. Based on the most recent work [7] analytically located TCPs, we obtain the two relevant length scales as functions of the power-law exponent α. As a result, we propose an extended finite-size scaling (FSS) theory of the GEP, incorporating both dynamic and static aspects of tricritical phenomena. It is notable that for strong heterogeneity ($2 < \alpha < 3$). The results also indicate a nonzero fraction of infected nodes even in the limit of vanishing infection probability, reported in Ref. [7].

This paper is organized as follows. We describe the GEP and show its phase diagram where the TCPs are drawn as a function of α in Sec. II, where the network basic properties are discussed as well. In Sec. III, the extended FSS theory is summarized with the conjecture

*E-mail: msha@chosun.ac.kr

of two relevant length scales and crossover scaling behaviors, which is numerically confirmed. We conclude this paper with summary and some remarks in Sec. IV.

II. Model

The GEP on networks is implemented as follows. At every instant, a node is in one of the four states: unexposed ($\mathbf{S_1}$), exposed ($\mathbf{S_2}$), infected ($\mathbf{I}$), and removed ($\mathbf{R}$). Initially only a single node (the "seed") is in the $\mathbf{I}$-state, while the others are all in the $\mathbf{S_1}$-state. At every time step, a randomly chosen $\mathbf{I}$-node attempts to infect all of its $\mathbf{S_1}$- or $\mathbf{S_2}$-neighbors, each of the former (latter) with an independent and identical probability λ (μ). The neighbors which have been successfully infected turn into $\mathbf{I}$-nodes, and the $\mathbf{S_1}$-neighbors which remain uninfected become $\mathbf{S_2}$-nodes. After then the $\mathbf{I}$-node immediately deactivates by changing its state permanently to $\mathbf{R}$, no longer participating in the process. The same procedure is repeated until the network runs out of $\mathbf{I}$-nodes. In the special case $\mu = \lambda$, the process is equivalent to the susceptible-infected-removed (SIR) model [15], a dynamic version of the bond percolation model. If the network consists of N nodes and in the end there are R nodes in the $\mathbf{R}$-state, the fraction $r \equiv R/N$ is chosen to be the order parameter, so that a phase transition occurs when r changes from zero to a positive value as λ is varied. The transition point $\lambda = \lambda_c$ is also called the *epidemic threshold*.

Tree-like description of the GEP. — An ensemble of random scale-free networks is generated by a degree distribution $p_k = k^{-\alpha}/\zeta_\alpha$, where the degree k of each node can be any integer not less than the minimum degree k_m, and the Hurwitz zeta function $\zeta_s \equiv \sum_{k=k_m}^{\infty} k^{-s}$ gives the normalization constant. The degrees of adjacent nodes are assumed to be uncorrelated. Moreover, the power-law exponent α is assumed to be larger than 2, so that the average degree $\langle k\rangle = \zeta_{\alpha-1}/\zeta_\alpha$ is a finite number, which are *locally tree-like*, in the sense that they rarely contain loops made of a finite number of links [16]. A network with this property can be decomposed into separate layers of nodes, each layer index n indicating the distance from the seed.

In order to keep track of the spreading, we consider the probability q_l that a node in the l-th layer, reached by following a randomly chosen link, ends up in the $\mathbf{R}$-state. Utilizing the tree-like property, the probability $1-q_{l+1}$ of a node in the $(l+1)$-th layer being uninfected is related to the corresponding probability in the l-th layer by a recursive relation

$$1-q_{l+1} = \sum_{k=k_m}^{\infty} p'_k \Bigg[(1-q_l)^{k-1} + \sum_{n=1}^{k-1} \binom{k-1}{n} (1-\lambda)(1-\mu)^{n-1} q_l^n (1-q_l)^{k-1-n} \Bigg], \quad (1)$$

where $p'_k \equiv k p_k/\langle k\rangle$ is the degree distribution, weighted by k because higher-degree nodes are more likely to be chosen. The first term in the summand represents the case when none of the neighbors in the l-th layer are infected, and the second term corresponds to the case when all of the n infected neighbors fail to pass on contagion. Calculating the sums, Eq. (1) leads to a discrete map

$$q_{l+1} = f(q_l). \quad (2)$$

If $q_\infty = \lim_{l\to\infty} q_l$, the order parameter r satisfies

$$1-r = \sum_{k=k_m}^{\infty} p_k \Bigg[(1-q_\infty)^{k} + \sum_{n=1}^{k} \binom{k}{n} (1-\lambda)(1-\mu)^{n-1} q_\infty^n (1-q_\infty)^{k-n} \Bigg]. \quad (3)$$

For $q_\infty \ll 1$, the above equation implies

$$r = \langle k\rangle \lambda q_\infty + O\left(q_\infty^{\min[2,\alpha-1]}\right). \quad (4)$$

Thus the transition point coincides with the boundary between the $q_\infty = 0$ and $q_\infty > 0$ regimes.

Since we are interested in the near-TCP properties of the GEP, we focus on the behavior of $f(q_l)$ for $q_l \ll 1$, which is described by the Taylor expansion

$$\begin{aligned} f(q_l) = {} & \frac{\zeta_{\alpha-2}-\zeta_{\alpha-1}}{\zeta_{\alpha-1}} \lambda q_l \\ & + \frac{\zeta_{\alpha-3}-3\zeta_{\alpha-2}+2\zeta_{\alpha-1}}{2\zeta_{\alpha-1}} g_2(\lambda,\mu) q_l^2 \\ & + \frac{\zeta_{\alpha-4}-6\zeta_{\alpha-3}+11\zeta_{\alpha-2}-6\zeta_{\alpha-1}}{6\zeta_{\alpha-1}} g_3(\lambda,\mu) q_l^3 \\ & + \frac{\Gamma(2-\alpha)}{\zeta_{\alpha-1}} g_{\alpha-2}(\lambda,\mu) q_l^{\alpha-2} + O\left(q_l^{\min[4,\alpha-1]}\right). \end{aligned} \quad (5)$$

Here Γ is the Gamma function and

$$g_s(\lambda,\mu) \equiv \frac{\mu-\lambda-(1-\lambda)\mu^s}{1-\mu}. \quad (6)$$

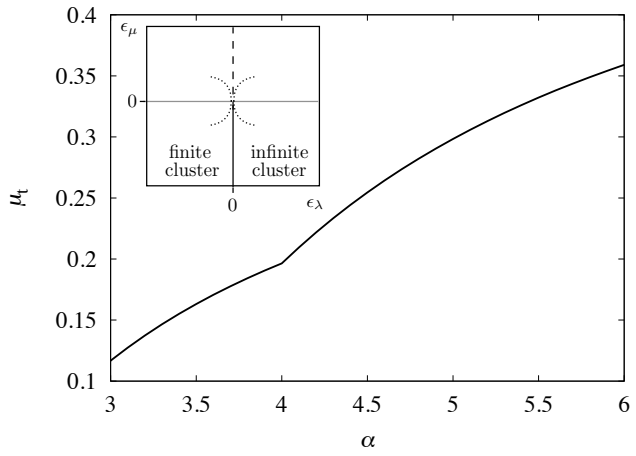

Fig. 1. The tricritical point (TCP) μ_t is plotted as a function of the power-law exponent α at the epidemic threshold. The inset shows the phase diagram in the vicinity of a TCP for a given value of $\alpha > 3$, where the solid (dashed) line indicates the continuous (discontinuous) transition line. The dotted lines represent the crossover scales given by $|\epsilon_\mu| \sim |\epsilon_\lambda|^\phi$.

Table 1. Scaling exponents of GEP on random scale-free networks of degree distribution $P(k) \sim k^{-\alpha}$.

	β_t	β_c	τ	d_l	ϕ	$\bar{\nu}_t$
$\alpha > 5$	$\frac{1}{2}$	1	$\frac{5}{2}$	2	$\frac{1}{2}$	$\frac{5}{2}$
$4 < \alpha < 5$	$\frac{1}{\alpha-3}$	1	$\frac{5}{2}$	2	$\frac{\alpha-4}{\alpha-3}$	$\frac{2\alpha-5}{\alpha-3}$
$3 < \alpha < 4$	1	$\frac{1}{\alpha-3}$	$\frac{2\alpha-3}{\alpha-2}$	$\frac{\alpha-2}{\alpha-3}$	$4-\alpha$	$\frac{2\alpha-5}{\alpha-3}$
$2 < \alpha < 3$	$\frac{4-\alpha}{3-\alpha}$	$\frac{1}{3-\alpha}$	–	–	–	–

Note that q_l^s with integer s represents the contribution from infection attempts involving s neighbors. On the other hand, $q_l^{\alpha-2}$ corresponds to contributions from *hubs*, whose effects become stronger with decreasing α. It is clear that μ contributes only to infection attempts involving more than 2 neighbors.

III. Numerical Results

TCP Identification — We focus on the case when α has a noninteger value greater than 3. For a given value of α satisfying this condition, we can always identify the dominant components of $f(q_l)$. This, together with the approximation $d_l q_l \simeq q_{l+1} - q_l$ for Eqs. (2) and (5), gives

$$d_l q_l \simeq \epsilon_\lambda q_l + u_\alpha \epsilon_\mu q_l^{1+1/\beta_c} - v_\alpha q_l^{1+1/\beta_t} . \qquad (7)$$

Here u_α and v_α are α-dependent positive coefficients, the dimensionless parameters $\epsilon_\lambda \equiv (\lambda - \lambda_c)/\lambda_c$ and $\epsilon_\mu \equiv (\mu - \mu_t)/\mu_t$ are defined in terms of

$$\lambda_c = \frac{\zeta_{\alpha-1}}{\zeta_{\alpha-2} - \zeta_{\alpha-1}} = \frac{\langle k \rangle}{\langle k(k-1) \rangle} \text{ for } \alpha > 3 \qquad (8)$$

and a nonzero solution μ_t of

$$g_2(\lambda_c, \mu_t) = 0 \text{ for } \alpha > 4,$$
$$g_{\alpha-2}(\lambda_c, \mu_t) = 0 \text{ for } 3 < \alpha < 4. \qquad (9)$$

The α-dependence of μ_t is illustrated in Fig. 1, with the switching at $\alpha = 4$ manifest as a cusp singularity. Finally, β_c and β_t are α-dependent exponents, whose values are listed in Table 1. A phase transition occurs when the fixed-point equation $d_l q_l = 0$ has an unstable fixed point at $q_l = 0$ and a stable fixed point at $q_l > 0$, so that a positive q_0 in the initial state can saturate to $q_\infty > 0$ as l is increased. For $\epsilon_\lambda < 0$, Eq. (7) is approximated as $d_l q_l \simeq -|\epsilon_\lambda| q_l$, which implies an exponential decay $q_l \sim \exp(-|\epsilon_\lambda| l)$ to $q_\infty = 0$. Thus the contagion remains localized to a λ-dependent length scale $l_\lambda \sim |\epsilon_\lambda|^{-1}$. In contrast, if $\epsilon_\lambda > 0$, the contagion initially spreads as $q_l \sim \exp(\epsilon_\lambda l)$ and eventually saturates to a positive value

$$q_\infty \simeq \begin{cases} [\epsilon_\lambda/(u_\alpha|\epsilon_\mu|)]^{\beta_c} & \text{if } \epsilon_\mu < 0, \\ [\epsilon_\lambda/v_\alpha]^{\beta_t} & \text{if } \epsilon_\mu = 0, \\ [u_\alpha \epsilon_\mu / v_\alpha]^{\beta_c \beta_t/(\beta_c - \beta_t)} & \text{if } \epsilon_\mu > 0. \end{cases} \qquad (10)$$

This implies that, if λ_c obtained from Eq. (8) satisfies $0 < \lambda_c < 1$ (this is true if k_m is sufficiently large), the transition point (*epidemic threshold*) is given by $\lambda = \lambda_c$. Using Eq. (10) as well as Eq. (4), we observe that for $\epsilon_\mu < 0$ the transition is continuous, with $r \sim \epsilon_\lambda^{\beta_c}$ in its vicinity. The critical exponent β_c is equal to that of the bond percolation (or the ordinary SIR model) on scale-free networks [17]. In contrast, for $\epsilon_\mu > 0$ a discontinuous transition occurs. The marginal case $\epsilon_\mu = 0$ corresponds to a TCP, with $r \sim \epsilon^{\beta_t}$ in its vicinity.

In Table 1, the tricritical exponent β_t is always smaller than β_c, reflecting more rapid increase of r from zero aided by μ. For a given value of $\alpha > 3$, the phase diagram is illustrated in the inset of Fig. 1.

Divergent length scales. — There are the two length scales which diverge at $\epsilon_\mu = 0$. We note that Eq. (7) remains invariant under the rescaling $l \to bl$ if the other variables rescale as

$$q_l \to b^{-\beta_t} q_{bl}, \quad \epsilon_\lambda \to b^{-1} \epsilon_\lambda, \quad \epsilon_\mu \to b^{-\phi} \epsilon_\mu, \qquad (11)$$

where the crossover scaling exponent $\phi \equiv 1 - \beta_t/\beta_c$.

The rescaling behavior of ϵ_λ reflects the diverging length scale $l_\lambda \sim |\epsilon_\lambda|^{-1}$. Similarly, the rescaling behavior of ϵ_μ implies another divergent length scale $l_\mu \sim |\epsilon_\mu|^{-1/\phi}$. Near TCPs ($\epsilon_\mu = 0$), the spreading is governed by whichever of l_λ and l_μ is larger. For $l_\lambda \gg l_\mu$, the **R**-cluster exhibits fractal properties of ordinary bond percolation. For $l_\lambda \ll l_\mu$, the **R**-cluster shows properties which are fractal but still distinct from ordinary bond percolation. The boundaries between these two regimes are given by the crossover scale $|\epsilon_\mu| \sim |\epsilon_\lambda|^\phi$, which is marked in the inset of Fig. 1 by dotted lines.

Extended FSS theory. — To describe the effects of N, we take into account the rescaling

$$N \to b^{-\bar{\nu}_t} N \tag{12}$$

in addition to Eq. (11). The value of $\bar{\nu}_t$ is obtained by the following heuristic arguments: First, at TCP the distribution of of finite **R**-clusters obeys a power law $P_R \sim R^{-\tau+1}$, where R denotes the number of nodes in the cluster. Since the network is locally tree-like, μ does not affect the properties of finite clusters. Thus the Fisher exponent τ is simply given by that of the ordinary bond percolation [17], see Table 1. The size of the largest cluster is given by $Nr \sim N^{1+\beta_t/\bar{\nu}_t}$ at the tricritical point. Then $\int_{Nr}^{\infty} P_R \, \mathrm{d}R = P_\infty$, where P_∞ is the probability of percolation. Due to the tree-like structure of the network, the formation of a percolating cluster is driven only by λ. Thus, even at the tricritical point, P_∞ is governed by the critical exponent β_c as $P_\infty \sim N^{-\beta_c/\bar{\nu}_t}$. The hyperscaling relation is as follows:

$$\bar{\nu}_t = \beta_t + \frac{\beta_c}{\tau - 2}, \tag{13}$$

from which we derive $\bar{\nu}_t$ shown in Table 1.

Near a TCP, the interplay of l_λ, l_μ, and l_N gives rise to an extended finite-size scaling (FSS) form

$$q_l = l_N^{-\beta_t} \Phi_q(l/l_N, l_\lambda/l_N, l_\mu/l_N) \, . \tag{14}$$

In an actual simulation, the layer index l can be replaced with the time t, and instead of q_l it is easier to measure the mean infected cluster size $\langle R \rangle = \int_0^{Nr} R \, P_R \, \mathrm{d}R$, which implies $\langle R \rangle \sim N^{\gamma_t/\bar{\nu}_t}$ with

$$\gamma_t = 1 - \frac{\beta_t + \beta_c}{\bar{\nu}_t}. \tag{15}$$

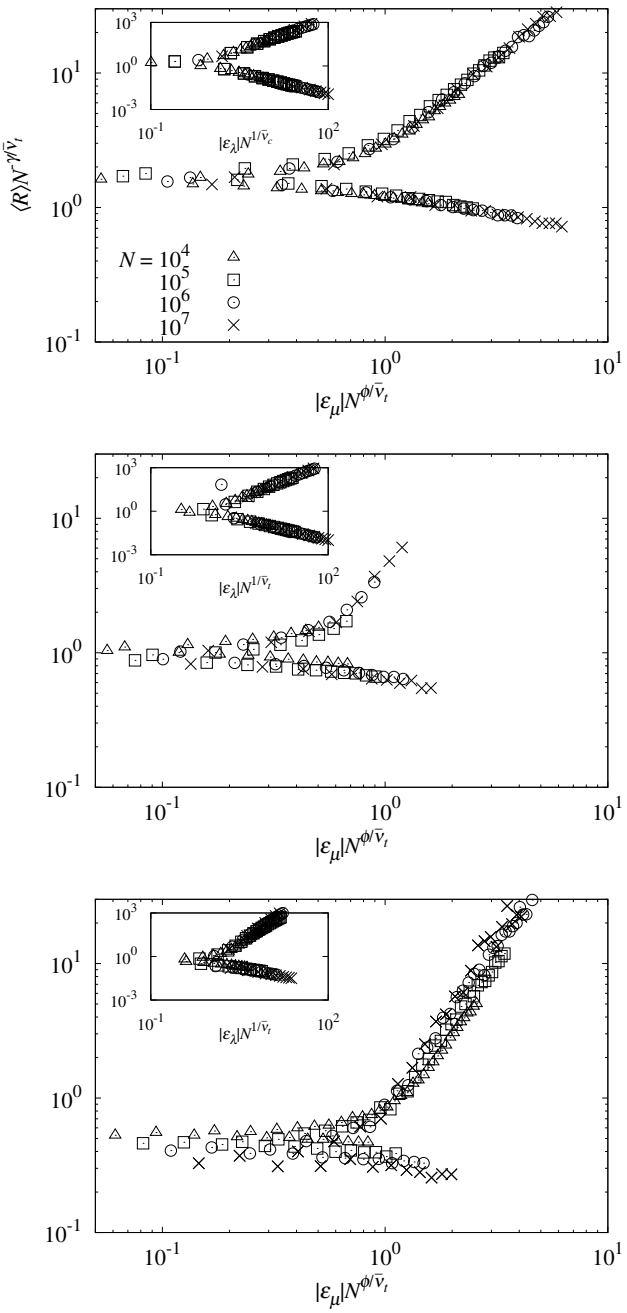

Fig. 2. In the steady-state limit, we show the finite-size scaling (FSS) forms of the mean infected cluster size $\langle R \rangle$, given by Eq. (16) with $t = \infty$ and $\epsilon_\lambda = 0$ for random scale-free networks with $\alpha = 5.5$ (top), 4.5 (middle) and 3.5 (bottom), respectively. The insets correspond to the cases of $\epsilon_\mu = 0$.

Using this exponent together with Eqs. (11) and (12), we can construct another FSS form

$$\langle R \rangle = N^{\gamma_t/\bar{\nu}_t} \Phi_{\langle R \rangle} \left(t N^{-1/\bar{\nu}_t}, \epsilon_\lambda N^{1/\bar{\nu}_t}, \epsilon_\mu N^{\phi/\bar{\nu}_t} \right). \tag{16}$$

We numerically confirm the FSS forms of $\langle R \rangle$ in the final state, given by Eq. (16) as $t \to \infty$ and $\epsilon_\lambda = 0$, see

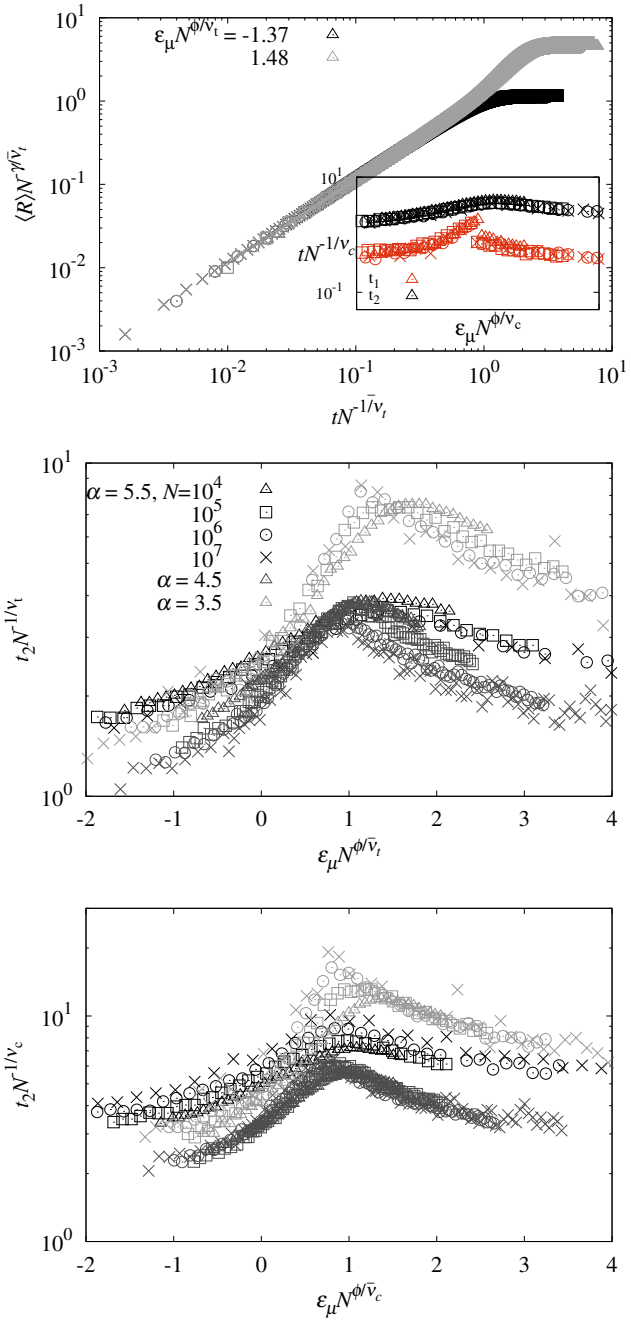

Fig. 3. (Color online) In the left panel, we plot the extended FSS forms of $\langle R\rangle$ as a function of the rescaled time $tN^{1/\bar{\nu}_t}$ below (positive, black) and above (negative, gray) the tricriticality for the case of $\alpha = 5.5$, the inset of which shows the FSS behaviors of t_1 (black) and t_2 (red) for all the ranges of ϵ_μ with respect to the normalized distance to $\epsilon_\mu N^{\phi/\bar{\nu}_c}$. In the middle and right panels, the data collapse of $t_2 N^{-1/\bar{\nu}_i}$ against $\epsilon_\mu N^{\phi/\bar{\nu}_i}$ is checked for the tricritical exponent $\bar{\nu}_t$ (middle) and the critical exponent $\bar{\nu}_c$ (bottom), respectively.

Fig. 2, which are random scale-free networks with $\alpha = 5.5$ (top), 4.5 (middle), and 3.5 (bottom), respectively. The insets of Fig. 2 show the FSS forms for $\epsilon_\mu = 0$.

In Fig. 3, we also numerically test the extended FSS theory of the time evolution of $\langle R\rangle$ as plotting below and above in the thermodynamic limit where $N \to \infty$. In particular to the FSS form of the characteristic time scales t_1 (the correlation time of the ordinary percolation) and t_2 (that of TCPs). How to indicate them is shown in the left panel of Fig. 3. For the cases of $\alpha = 5.5$, 4.5, and 3.5, in the middle and right panels of Fig. 3, the extended FSS therory of t_2 is checked as data collapsing for the tricritical exponent $\bar{\nu}_t$ (middle) and the critical one $\bar{\nu}_c$ (bottom), respectively.

IV. Summary and discussion

We proposed the extended finite-size scaling (FSS) theory of the generalized epidemic process (GEP) on uncorrelated random scale-free networks with $p_k \sim k^{-\alpha}$ and numerically confirmed associated scaling exponents against α as well as crossover scalings. Numerical studies for $2 < \alpha < 3$ needs to some additional study related to cutoff-degree scalings because such cases are very sensititve to degree-degree correlations and finite-size effects, which is an important future work.

ACKNOWLEDGEMENTS

This research was supported by Basic Science Research Program through the National Research Foundation of Korea (NRF)[Grant No. NRF-2017R1D1A3A03000578]. Some results presented here grew out an enjoyable collaboration with Kihong Chung, Yongjoo Baek, and Daniel Kim in the early stage of our study for the GEP on random scale-free networks [7].

REFERENCES

[1] D. Centola, Science **329**, 1194 (2010).

[2] M. Singer, *Introduction to Syndemics: A Critical Systems Approach to Public and Community Health* (Wiley, Hoboken, 2009).

[3] R. Cohen and S. Havlin, *Complex networks: structure, robustness and function* (Cambridge University Press, Cambridge, 2010).

[4] S. N. Dorogovtsev, A. V. Goltsev and J. F. F. Mendes, Phys. Rev. Lett. **96**, 040601 (2006).

[5] G. J. Baxter, S. N. Dorogovtsev, A. V. Goltsev and J. F. F. Mendes, Phys. Rev. E **83**, 051134 (2011).

[6] D. J. Watts, Proc. Natl. Acad. Sci. USA **99**, 5766 (2002).

[7] Y. Baek, K. Chung, M. Ha, H. Jeong and D. Kim, Phys. Rev. E **99**, 020301 (2019).

[8] W. Cai, L. Chen, F. Ghanbarnejad, and P. Grassberger, Nat. Phys. **11**, 936 (2015).

[9] P. Grassberger, L. Chen, F. Ghanbarnejad and W. Cai, Phys. Rev. E **93**, 042316 (2016).

[10] W. Choi, D. Lee, J. Kertész and B. Kahng, Phys. Rev. E **98**, 012311 (2018).

[11] S. Lübeck, J. Stat. Phys. **123**, 193 (2006).

[12] P. Grassberger, J. Stat. Mech. **2006**, P01004 (2006).

[13] E. K. Riedel, Phys. Rev. Lett. **28**, 675 (1972).

[14] E. K. Riedel and F. J. Wegner, Phys. Rev. B **9**, 294 (1974).

[15] W. O. Kermack, A. G. McKendrick, Proc. R. Soc. Lond. A Math. Phys. Sci. **115**, 700 (1927).

[16] B. Bollobas, *Random graphs* (Academic Press, New York, 1985)

[17] R. Cohen, D. ben-Avraham and S. Havlin, Phys. Rev. E **66**, 036113 (2002).